Stability Control of Autonomous Ground Vehicles Using Control-Dependent Barrier Functions

Yiwen Huang, Sze Zheng Yong, *Member, IEEE*, and Yan Chen, *Member, IEEE*

***Abstract*—In the development of autonomous ground vehicles (AGVs), guaranteeing vehicle driving safety is a major concern. Among various aspects that need to be thoughtfully considered for driving safety, vehicle stability is one of the most fundamental and important factors. In this paper, to describe a guaranteed vehicle stability control problem, a new time-varying control-dependent invariant set is introduced. Correspondingly, the concept of a time-varying control-dependent barrier function (CDBF) is proposed. The proposed time-varying CDBF is more general than conventional control barrier functions (CBF), since we additionally consider invariant sets that can be time-varying and control-dependent, which will have broader applications. Then, using the proposed framework, we design a vehicle stability control algorithm, which guarantees that the vehicle states are always kept in the time-varying and control-dependent lateral stability regions. Finally, the correctness and effectiveness of the proposed theory and control method are verified and discussed through illustrative simulation results of high-speed J-turn and double lane change maneuvers for an AGV.**

***Index Terms*—Control-dependent barrier functions, autonomous ground vehicles, vehicle stability control, four-wheel steering, safety control.**

I. Introduction

ADVANCED autonomous driving technologies bring new opportunities to enhance the safety and efficiency of vehicle and transportation systems [1]. Currently, various advanced driver assistance systems (ADAS) are being developed to make vehicles safer to drive. For example, the integration of lane-keeping assist system (LKAS) and adaptive cruise control (ACC) enables the attainment of level 2 (SAE J3016 [2]) autonomous driving in many driving scenarios. However, when facing certain critical driving situations, the existing ADAS are not capable enough of ensuring vehicle safety due to the lack of effective vehicle dynamics controls, which makes the realization of the full autonomous driving at level 5 an even more challenging task. Therefore, in addition to the perception and planning systems, a well-developed vehicle control system, which guarantees vehicle driving stability, becomes very necessary for all levels of autonomous driving.

Vehicle stability region, or in general, the stability region of a dynamical system, can often be described by one or multiple stability constraints. Thus, the goal of stability control is to guarantee that all the stability constraints are satisfied at all times under any conditions. To achieve such a control goal, various methods, such as model predictive control [3] and dynamic window approach [4] were proposed and evaluated. Inspired by the barrier certificate [5], [6] and invariant set [7], the control barrier function (CBF) [8] is another effective method to guarantee system stability in a simpler and more computationally-efficient manner. Generally, the conventional CBF can be divided into two categories, namely the reciprocal CBF (RCBF) [9]–[14] and the zeroing CBF (ZCBF) [9], [15], [16]. The RCBF has an infinite value when the system states are on the set boundary, which may cause unbounded control efforts. On the other hand, the ZCBF becomes zero when the states are on the set boundary. Using CBF (either RCBF or ZCBF), control laws can be designed to ensure the system states always stay within a defined stability/safety set. Thus, the invariance of the stability/safety set, more precisely, a controlled invariant set, can be guaranteed. CBF has been utilized to solve safety control problems for autonomous ground vehicles (AGVs) and other mobile systems, such as lane-keeping [9], [17], adaptive cruise control [9], [17], obstacle avoidance [18], and collision-free multi-robot systems [19]. To simultaneously achieve tracking (or stabilizing) and safety control, CBF can also be integrated with control Lyapunov functions (CLF) as well as other tracking control methods [9], [17], [20]–[23]. In [24] and [25], the control Lyapunov-barrier function (CLBF) was successfully combined with MPC for both stability and safety control. Further, in some cases when a safety set is time-varying or dynamic, the time-varying barrier Lyapunov functions (BLF) [12], time-varying CBF [26] and invariant control with dynamic constraints [27] were proposed and utilized to tackle related safety control problems.

To our best knowledge, CBF has never been used to guarantee the controlled invariance of a stability region. More importantly, since the stability region in vehicle control problems is defined by constraints that are control-dependent, the existing conventional controlled invariant set concept is not directly suitable to describe such a stability region/set, and the corresponding CBFs cannot properly resolve the associated control problems. For example, in a region-based stability control problem for AGVs, the vehicle stability set is typically defined with respect to both time-varying variables (e.g., a desired longitudinal speed and/or

Manuscript received May 14, 2020; revised August 20, 2020 and December 10, 2020; accepted January 22, 2021. Date of publication February 9, 2021; date of current version November 23, 2021. This work was supported in part by the National Science Foundation Grant CNS-1943545. *(Corresponding author: Yan Chen.)*

Yiwen Huang and Sze Zheng Yong are with the School for Engineering of Matter, Transport and Energy, Arizona State University, Tempe, AZ 85281 USA (e-mail: yiwenhuang@asu.edu; szyong@asu.edu).

Yan Chen is with the Polytechnic School, Arizona State University, Tempe, AZ 85281 USA (e-mail: yanchen@asu.edu).

Color versions of one or more figures in this article are available at https://doi.org/10.1109/TIV.2021.3058064.

Digital Object Identifier 10.1109/TIV.2021.3058064

a reference path) and control inputs (e.g., a feedback steering angle). Based on the authors' previous study [28] and a similar observation in [29], as the vehicle longitudinal speed and steering angle (front and/or rear) change, the size and location of the vehicle lateral stability region also change. Namely, the vehicle lateral stability region, which is selected as a controlled invariant set, is actually both time-varying and control-dependent. In this paper, to handle the region-based stability control problem for AGVs, where the vehicle states are required to be always inside a stability region (see an example of vehicle dynamics in [30]), a novel *time-varying control-dependent* (TVCD) invariant set and the corresponding time-varying *control-dependent barrier function* (CDBF) are proposed and studied.

A preliminary study of the control-dependent invariant set and CDBF was presented in the authors' conference paper [31], and this paper contains three additional contributions. First, the definition of the invariant set is extended to be both time-varying and control-dependent. Second, a novel integral control strategy is proposed and a corresponding new framework of time-varying CDBF is proposed with rigorous proofs. Third, a more realistic region-based vehicle lateral stability control problem based on nonlinear vehicle and tire models is formulated, in contrast to the linear models utilized in [31]. In addition, more simulation scenarios are considered to verify the correctness and effectiveness of the proposed theory and control methods.

The remainder of this paper is organized as follows. In section II, the concept of a TVCD invariant set is presented. In section III, the proposed time-varying CDBF is defined and the corresponding proofs are presented in detail. In section IV, based on the proposed time-varying CDBF, a stability control problem for vehicle lateral dynamics is formulated. The simulation results are presented and discussed in section V. Concluding remarks are given in section VI.

Notation: A continuous function $\alpha : [0, a) \to [0, \infty)$ is said to belong to class *K* if it is strictly increasing and $\alpha(0) = 0$. A continuous function $\alpha : (-a, b) \to (-\infty, \infty)$is said to belong to extended class *K* for positive *a* and *b* if it is strictly increasing and $\alpha(0) = 0$ [32]. A continuous function $\sigma : [0, a) \times [0, \infty) \to [0, \infty)$ is said to belong to class *KL* if, for each fixed s, the mapping $\sigma(r, s)$ belongs to class *K* with respect to *r* and, for each fixed *r*, the mapping $\sigma(r, s)$ is decreasing with respect to *s* and $\sigma(r, s) \to 0$ as $s \to \infty$ [32].

In this paper, the first-order Lie derivative of a scalar function $h(x) : \mathbb{R}^n \to \mathbb{R}$ in the direction of $f(x) = [f_1(x), \cdots, f_n(x)]^T$ is, as in [33], given by

$$L_f h\left(x\right) = \sum_{k=1}^{n} f_k\left(x\right) \frac{\partial h\left(x\right)}{\partial x_k} . \tag{1}$$

II. Time-Varying Control-Dependent Invariant Set

In this section, for the sake of completeness, the concepts of invariant set and controlled invariant set are first reviewed in the following Definition 1 and 2, respectively. Then, the novel concept of a TVCD invariant set is introduced.

Definition 1 [7]: A set $\psi \subset \mathbb{R}^n$ is said to be *positively invariant* with respect to a nonlinear system

$$\dot{x} = f\left(x\right), \tag{2}$$

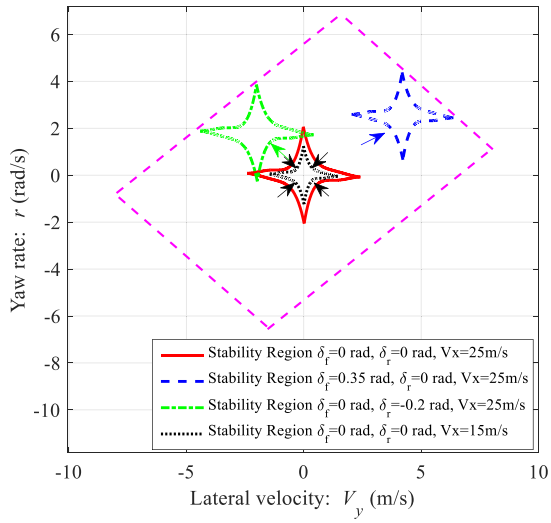

Fig. 1. Variations of the vehicle lateral stability region with respect to control inputs (δ_f and/or δ_r) and time-varying parameters (V_x).

where $x \in \mathbb{R}^n$ is the system state vector, if for any $t_0 \geq 0$ and all $x(t_0) \in \psi$, the solution $x(t) \in \psi$ for $t > t_0$.

Remark 1: The positive invariance of a set implies that the system states always remain in the set for all times. A positively invariant set is also commonly called as a forward invariant set. Unless otherwise specified, we will simply refer to positively/forward invariant sets as invariant sets in the remainder of this paper as a shorthand.

Definition 2 [7]: Consider a nonlinear control system of the form

$$\dot{x} = f\left(x, u\right), \tag{3}$$

where $x \in \mathbb{R}^n$ and $u \in \mathbb{R}^m$are the system state and control input, respectively.[1] The set $\psi \subset \mathbb{R}^n$ is said to be *controlled invariant* with respect to (3), if, for any $t_0 \geq 0$ and all $x(t_0) \in \psi$, there exists a feedback control law $u = \phi(x)$, which assures the existence and uniqueness of the solution $x(t) \in \psi$ for $t > t_0$.

Remark 2: In Definition 2, although the set, ψ, is controlled to be invariant with a properly designed control u, the set itself is independent of u.

The (controlled) invariant set concept was usually applied to guarantee the safety of dynamic systems [9], [15], [26]. For control problems with safety sets defined only by system states, the controlled invariant set in Definition 2 is useful for control design. However, for control problems with safety sets defined by time-varying and control-dependent variables, the above definitions may not be directly applicable.

For example, in the vehicle lateral stability control problem, the control objective is to always keep vehicle states (e.g., yaw rate and lateral velocity) within an estimated or a defined stability region [34], [35]. Such a stability region depicts the vehicle directional stability (e.g., neither oversteering nor too understeering) by analyzing both vehicle and tire stability [30]. In the authors' previous study [28], as shown in Fig. 1, the vehicle lateral stability region was found to shift with respect to the front

[1]The signals x and u are functions of time t, but for brevity, this explicit dependence is omitted throughout the paper when it is clear from context.

(δ_f) and/or rear (δ_r) wheel steering angles. In addition, when the longitudinal velocity (V_x) changes, the size of the stability region also changes although the shape almost remains the same. For lateral dynamics control of AGVs, the vehicle longitudinal velocity and/or the front wheel steering angle are often given by a high-level path planner as reference or feedforward signals (but not system states) that are time-varying. Meanwhile, additional front and/or rear wheel steering angles, actuated by active steering systems, are typically added as feedback control inputs [37]. Therefore, the vehicle lateral stability region in Fig. 1, if defined or selected as an invariant set, is both time-varying and control-dependent.

Remark 3: Although the specific shapes and areas of vehicle lateral stability regions in Fig. 1 were originally estimated in the authors' previous work by considering both vehicle and tire stabilities [28], [30], the general shrinking/expanding and shifting features of lateral stability regions with respect to steering angles and the vehicle longitudinal speed were also observed and well-documented in literature [29], [39], [40].

Moreover, the (ground) front and rear wheel steering angles are assumed, without loss of generality, to have limits $\delta_f \in [-0.35 \text{ rad}, 0.35 \text{ rad}]$ and $\delta_r \in [-0.2 \text{ rad}, 0.2 \text{ rad}]$, respectively, and the maximum vehicle longitudinal speed is $V_x = 25$ m/s (these parameters can be easily changed to get different stability regions). Thus, an extended envelope of stability regions can be defined by the area outlined by pink dashed lines in Fig. 1 based on the stability region shifting and shrinking/expanding feature, no matter how the steering angles and longitudinal speed change within the limits. This enveloped area, as a set consisting of all the possible stability regions, is a time-invariant and control-independent set, which could be described by the existing concept of the controlled invariant set in Definition 2. However, the invariance of the whole enveloped area does not necessarily imply the invariance of the shifted and shrunk/expanded stability regions as the subsets, which are discussed more in Remark 4. Therefore, to describe such an invariance set that is time-varying and control-dependent, a new concept is introduced as follows.

Definition 3: Consider a nonlinear control system in (3), a set $\psi(u,t) \subset \mathbb{R}^n$ is said to be time-varying and control-dependent (TVCD) invariant if there exist a control $u \in U$ and a $u_0 \in U$ such that for any $t_0 \geq 0$ and all $x(t_0) \in \psi(u_0, t_0)$, $x(t) \in \psi(u,t)$ for all $t \in T = [t_0, t_{end})$, where $U \subset \mathbb{R}^m$ is the vector space or set of all feasible u.

Remark 4: In Definition 3, $T = [t_0, t_{end})$ is the maximum time interval that the set can be guaranteed to be TVCD invariant. Note that for any time intervals in T, if the controlled invariant set does not change with time, a TVCD invariant set becomes a control-dependent invariant set [31]. For the set $\psi(u,t)$ in Definition 3, a set $\psi = \cup_{u \in U, t \in T} \psi(u,t)$, which is a union of all possible $\psi(u,t)$ for any $u \in U$ and $t \in T$, could be a controlled invariant set with a properly designed control u [15], [26]. However, since the $\psi(u,t)$ is a subset of ψ, a control u, which makes ψ controlled invariant, does not necessarily make the subset $\psi(u,t)$ TVCD invariant. On the contrary, a control u, which makes each subset $\psi(u,t)$ TVCD invariant, can sufficiently make the set ψ controlled invariant since $\psi(u,t) \subseteq \psi$. Therefore, the determination of the control u that makes the set $\psi(u,t)$ TVCD invariant is different from the determination of u in Definition 2.

Inspired by an AGV lateral stability control problem, the necessity and definition of a new concept on a TVCD invariant set is proposed for general dynamic systems. The application of the new concept in system control design is discussed in the next section.

III. Time-Varying Control-Dependent Barrier Function

In this section, existing definitions of a barrier function (BF) and a CBF are first reviewed. Then, the new concept of a time-varying CDBF is introduced and the corresponding properties are described.

Based on the definitions of the invariant set and controlled invariant set, the corresponding BF and CBF were proposed to describe the conditions of an invariant set and a controlled invariant set, respectively [7], [9]. Generally, the BF corresponding to an invariant set is defined as follows.

Definition 4 [9]: Considering a nonlinear system in (2), a set ψ is defined by a continuously differentiable function $h(x) : \mathbb{R}^n \to \mathbb{R}$ as,

$$h(x) \geq 0, x \in \psi, \tag{4}$$

$$h(x) = 0, x \in \partial\psi, \tag{5}$$

$$h(x) > 0, x \in Int(\psi), \tag{6}$$

where $\partial\psi$ and $Int(\psi)$ denote the boundary and the interior of ψ , respectively. If there exists an extended class *K* function α [32], such that for all $x \in \psi$,

$$L_f h(x) \geq -\alpha(h(x)), \tag{7}$$

then the set ψ is an invariant set. $h(x)$ is called a zeroing barrier function (ZBF) [9]. The existence of ZBF is a sufficient and necessary condition for the invariance of ψ [9].

Inspired by the definition of the CBF for an affine control system in [9], the CBF for a general nonlinear control system is defined as follows.

Definition 5 (Extended from Definition 4 in [9]) Consider a nonlinear control system in (3) and a set ψ defined by (4)–(6) in Definition 4, if there exist a control u and an extended class *K* function α such that for all $x \in \psi$,

$$L_f h(x) + \alpha(h(x)) \geq 0, \tag{8}$$

then the ψ is a controlled invariant set and $h(x)$ is a zeroing CBF (ZCBF).

Note that although (7) have the same form as (8), the system function f in (8) is depicted by (3), which contains control input and thus makes (8) different from (7) when Lie derivatives are calculated.

If $h(x)$ is a CBF, any Lipschitz continuous control u that satisfies (8) will make the set ψ controlled invariant. Hence, the existence of CBF is sufficient for a set to be controlled invariant. Similar to the relationship between a BF and an invariant set, the existence of a control u and a ZCBF is both sufficient and necessary for ψ to be controlled invariant [9].

Following the definition of BF and CBF, the corresponding definition of a time-varying CDBF for the newly defined TVCD invariant set in Definition 3 is presented as follows.

Definition 6: Consider a nonlinear control system in (3), where u is differentiable with a Lipschitz continuous $\dot{u}$, e.g., $\dot{u} = \omega$ and $\omega \in \Omega(u)$, $\Omega \subset \mathbb{R}^m$. Let u be a new system state, then the system is augmented as

$$\dot{\hat{x}} \triangleq \begin{bmatrix} \dot{x} \\ \dot{u} \end{bmatrix} = \begin{bmatrix} f(x,u) \\ \omega \end{bmatrix} = \hat{f}(\hat{x}, \omega), \tag{9}$$

where $\hat{x} = [\, x^T \; u^T \,]^T$. For a TVCD set $\psi(u,t)$(Definition 3) defined by a continuous and differentiable function $h(\hat{x},t)$ as

$$h(\hat{x},t) \geq 0, \forall x \in \psi(u,t), \tag{10}$$

$$h(\hat{x},t) = 0, \forall x \in \partial\psi(u,t), \tag{11}$$

$$h(\hat{x},t) > 0, \forall x \in Int(\psi(u,t)), \tag{12}$$

if there exist a control $u \in U$, where $\dot{u} \in \Omega$, and an extended class *K* function α such that for all $x \in \psi(u,t)$,

$$L_{\hat{f}} h(\hat{x},t) + \alpha(h(\hat{x},t)) \geq 0, \tag{13}$$

where

$$\begin{aligned} L_{\hat{f}} h(\hat{x},t) &= \sum f(\hat{x}) \frac{\partial h(\hat{x},t)}{\partial \hat{x}, t} \\ &= \frac{\partial h(\hat{x},t)}{\partial x}^T \dot{x} + \frac{\partial h(\hat{x},t)}{\partial u}^T \dot{u} + \frac{\partial h(\hat{x},t)}{\partial t}, \end{aligned} \tag{14}$$

then the set $\psi(u,t)$ is a TVCD invariant set. $h(\hat{x},t)$ is a time-varying zeroing control-dependent barrier function (ZCDBF). Moreover, the solution $x(t), u(t)$ exists and is unique by Peano's Theorem [41].

Remark 5: When the invariance conditions in (14) are applied in the optimization problem, $\dot{u}$ is suggested to be the auxiliary control variable and u can be obtained by integrating $\dot{u}$, i.e., we are introducing an integral control action. The reasons are two-fold. First, by selecting $\dot{u}$ as the control variable, the continuity and differentiability of the formal control u can be guaranteed. Second, if $u$is selected as the control variable in optimization, $\dot{u}$ should be determined in advance or bounded to avoid extreme values, which may violate the invariance conditions in (13). In addition, by comparing with the authors' previous study [31] that selects u as the control variable, it was found that its control performance is limited and conservative because the variable $\dot{u}$ in (14) was simply replaced by their upper and lower limits in [31]. Therefore, $\dot{u}$ is suggested to be the control variable in CDBF. $\Omega(u)$ is defined to be control-dependent to ensure $u \in U$. (48) and (49) are illustrative examples to further clarify the selection of $\Omega(u)$.

Proposition 1: Given a nonlinear control system in (9) and a TVCD set defined by (10)–(12), if there exists a time-varying ZCDBF $h(\hat{x},t)$ defined on the set $\psi(u,t)$ in Definition 6, then $\psi(u,t)$ is a TVCD invariant set.

Proof: Following a similar proof procedure to [9] and based on some definitions in [7] and references therein, the complete proofs of Proposition 1 are provided in the Appendix. ■

Remark 6: The condition in (13) to make $\psi(u,t)$ TVCD invariant is more general than the condition in (8), which only makes ψ controlled invariant. The definition of the time-varying CDBF is different from the concept of time-varying CBF (TCBF) in the literature since the control input determined by the time-varying CDBF also has impacts on the stability/safety constraints. Differently, in TCBF, the stability/safety constraints could be time-varying but remain unchanged with respect to different control inputs. One can easily verify that if $h(\hat{x},t)$ is independent of u and time-invariant, the term $\frac{\partial h(\hat{x},t)}{\partial u}^T$ and $\frac{\partial h(\hat{x},t)}{\partial t}$ in (14) are eliminated. Thus, (13) is reduced to the same form as in (8). Further, to enable the invariance control via $\dot{u}$ in (14), $\frac{\partial h(\hat{x},t)}{\partial u}^T$ in Definition 6 is assumed to be non-zero.

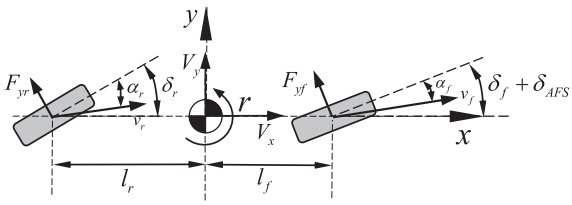

Fig. 2. Single-track 4WS vehicle model.

For a TVCD set described by (10)–(12), any control that satisfies the constraints (13) in Definition 6 will make the TVCD set invariant. Thus, a quadratic programming (QP) problem can be formulated to find a control derivative $\dot{u}$ (and the corresponding control u by integration) that satisfy one or multiple invariance constraints [15]. Since the QP is linear with respect to $\dot{u}$, the algorithm is real-time implementable without additional computational effort.

Note that although the proposed new concepts on the TVCD invariant set and time-varying CDBF are inspired by AGVs, these new concepts and theoretical work, including Proposition 1, are generally applicable to any other dynamic systems ((3) or (9)), whose safety or stability regions (constraints) are varying with respect to control and time. On that note, the vehicle dynamics and application are introduced in the next section.

IV. Guaranteed Vehicle Lateral Stability Control Using Time-Varying CDBF

For a four-wheel steering (4WS) vehicle equipped with two steer-by-wire systems, the steering angles of the front and rear wheels can be separately controlled by two steering motors. In this study, an AGV with a 4WS system is considered, in which both the front and rear wheel steering systems are adopted as the actuators (control inputs) to guarantee vehicle lateral stability (analogous to a safety specification). Selecting the lateral velocity and yaw rate as two system states, the single-track model of vehicle lateral dynamics, as shown in Fig. 2, is written as

$$\begin{aligned} \dot{V}_y + V_x r &= (F_{yf}\cos(\delta_f + \delta_{AFS}) + F_{yr}\cos\delta_r)/m_v \\ \dot{r} &= (l_f F_{yf}\cos(\delta_f + \delta_{AFS}) - l_r F_{yr}\cos\delta_r)/I_z, \end{aligned} \tag{15}$$

where m_v, I_z, δ_f, δ_{AFS}, and δ_r are the vehicle mass, yaw moment inertia, feedforward front steering angle, and feedback front and rear steering angles, respectively. V_x, V_y, and r are

the vehicle longitudinal velocity, lateral velocity, and yaw rate, respectively. l_f and l_r are the front and rear wheelbases, respectively. F_{yf} and F_{yr} are the lateral forces of the front and rear tires, which are calculated based on a nonlinear LuGre tire model as $F_y = f(\alpha_{f,\,r}, \lambda, F_n, \mu)$(see Appendix C) [38]. To calculate the lateral tire forces by the tire model, the tire slip angles are calculated in (16) and (17):

$$\alpha_f = [\delta_f(t) + \delta_{AFS}] - \tan^{-1}\left((V_y + l_f \cdot r)/V_x(t)\right), \quad (16)$$

$$\alpha_r = \delta_r - \tan^{-1}\left((V_y - l_r \cdot r)/V_x(t)\right), \quad (17)$$

where $\delta_f(t)$ and $V_x(t)$ are time-varying, given by either a driver or an upper-level feedforward control. The two feedback control inputs are selected as $u_1 = \delta_{AFS}$ and $u_2 = \delta_r$.

To describe the region-based vehicle lateral stability control problem using the proposed time-varying CDBF, the boundaries of the stability region are first formulated. In Fig. 1, taking the region depicted by the solid red curves as the stability set, which is estimated at a zero steering angle and a constant longitudinal velocity, the corresponding four boundaries are described by four independent functions as

$$h_1(x) = b_1(V_y) - r, \quad (18)$$

$$h_2(x) = b_2(V_y) - r, \quad (19)$$

$$h_3(x) = r - b_3(V_y), \quad (20)$$

$$h_4(x) = r - b_4(V_y), \quad (21)$$

where b_1, b_2, b_3, b_4 are the polynomial functions to describe the boundaries as $r = b_j(V_y), j = 1, 2, 3, 4$. However, the safety set defined by (18)–(21) is not enough to describe dynamic characteristics of the vehicle lateral stability region. Based on the authors' previous work [28], the region-based vehicle lateral stability control problem involves time-varying and control-dependent features, which are from the following two sources. First, when the front and rear steering angles are applied, the vehicle lateral stability region shifts along with specific directions [28], which is formulated in a shifting vector as

$$\vec{S} = \left[\, s_1(\delta_f(t), V_x(t), u_1, u_2)\ s_2(\delta_f(t), V_x(t), u_1, u_2) \,\right]^T, \quad (22)$$

where

$$s_1(\delta_f(t), V_x(t), u_1, u_2) = \frac{V_x(t)\left[l_r(\delta_f(t) + u_1) + l_f u_2\right]}{l_f + l_r}, \quad (23)$$

$$s_2(\delta_f(t), V_x(t), u_1, u_2) = \frac{V_x(t)\left[(\delta_f(t) + u_1) - u_2\right]}{l_f + l_r}. \quad (24)$$

Second, when the vehicle longitudinal velocity decreases or increases, the size of the stability region shrinks or expands correspondingly. Using the stability region estimated at $V_x = 25$m/s as a reference, a scaling function is derived to describe the size variation when V_x changes. Based on the characteristics of the stability region boundaries, the scaling functions are formulated separately for the different boundary pairs as shown in (25).

$$a_i(V_x(t)) = \begin{cases} k_1(V_x(t) - 25), & i = 1, 3 \\ k_2(V_x(t) - 25), & i = 2, 4 \end{cases}, \quad (25)$$

where k_1 and k_2 are the scaling factors. If $V_x < 25$ m/s, the stability region shrinks to be smaller (e.g., the region depicted by the black dotted curves in Fig. 1) than the reference region, and if $V_x > 25$ m/s, the stability region expands to be larger than the reference region. Note that the above time-varying feature is realized by setting the system parameters as time-varying variables. In more general cases, the stability/safety set can be explicitly dependent on time-varying variables.

Based on both the shifting vector and the scaling function, the four boundaries in (18)–(21) are reformulated as four time-varying and control-dependent functions in (26)–(29):

$$h_1(x, u, t) = b_1((V_y - s_1)) - (r - s_2) + a_1(V_x(t)), \quad (26)$$

$$h_2(x, u, t) = b_2((V_y - s_1)) - (r - s_2) + a_2(V_x(t)), \quad (27)$$

$$h_3(x, u, t) = (r - s_2) - b_3((V_y - s_1)) + a_3(V_x(t)), \quad (28)$$

$$h_4(x, u, t) = (r - s_2) - b_4((V_y - s_1)) + a_4(V_x(t)), \quad (29)$$

To sum up the problem description, since the shifting vector in (22) consists of two time-varying variables (δ_f and V_x) and two control inputs (u_1 and u_2), and the scaling function in (25) contains one time-varying variable (V_x), the guaranteed vehicle stability control problem using the stability region depicted in (26)–(29) is an instance of a TVCD invariant set as described in Definition 3. To resolve this control problem, the vehicle dynamic model in (15) is first augmented with the state vector as $\hat{x} = [\,V_y\ r\ u_1\ u_2\,]^T$,

$$\dot{\hat{x}} = \left[\,\dot{V}_y\ \dot{r}\ \dot{u}_1\ \dot{u}_2\,\right]^T = \left[\,f_1(\hat{x})\ f_2(\hat{x})\ \omega_1\ \omega_2\,\right]^T, \quad (30)$$

where f_1 and f_2 are the vehicle dynamics in (15), ω_1 and ω_2 are the control input dynamics that will be determined and discussed later.

Based on Definition 6, the vehicle stability region is defined as a TVCD invariant set C as follows:

$$C = \left\{x \in \mathbb{R}^2 \,|h_j(\hat{x}, t) \geq 0,\ j = 1, 2, 3, 4\right\}, \quad (31)$$

$$\partial C = \left\{x \in \mathbb{R}^2 \,|h_j(\hat{x}, t) = 0,\ j = 1, 2, 3, 4\right\}, \quad (32)$$

$$Int(C) = \left\{x \in \mathbb{R}^2 \,|h_j(\hat{x}, t) > 0,\ j = 1, 2, 3, 4\right\}, \quad (33)$$

Then, the set invariance conditions using the time-varying ZCDBF in (13) with respect to the stability region boundary functions in (26)–(29) are given by the following four constraints:

$$L_f h_j(\hat{x}, t) + \alpha_j(h_j(\hat{x}, t)) \geq 0, j = 1, 2, 3, 4, \quad (34)$$

where

$$L_f h_j(\hat{x}, t) = \frac{\partial h_j(\hat{x}, t)}{\partial V_y}\dot{V}_y + \frac{\partial h_j(\hat{x}, t)}{\partial r}\dot{r} + \frac{\partial h_j(\hat{x}, t)}{\partial u_1}\omega_1 + \frac{\partial h_j(\hat{x}, t)}{\partial u_2}\omega_2 + \frac{\partial h_j(\hat{x}, t)}{\partial t}, j = 1, 2, 3, 4. \quad (35)$$

Without loss of generality, we assume that the boundary functions $r = b_j(V_y), j = 1, 2, 3, 4$ are depicted by four linear functions as $r = b_j V_y + c_j, j = 1, 2, 3, 4$, where c_j are constants. Then, by substituting the shifting function in (22) and the scaling function in (25) into (26)–(29), the complete forms of the four time-varying and control-dependent boundary functions are rewritten as:

$$\begin{aligned} h_1(\hat{x},t) &= b_1 V_y - r \\ &+ \left[\frac{(1-b_1 l_r)}{l_f+l_r} V_x(t)\right] u_1 + \left[\frac{(-1-b_1 l_f)}{l_f+l_r} V_x(t)\right] u_2 \\ &+ \frac{(1-b_1 l_r)}{l_f+l_r}\delta_f(t) V_x(t) + a_1(V_x(t)), \end{aligned} \tag{36}$$

$$\begin{aligned} h_2(\hat{x},t) &= b_2 V_y - r + \left[\frac{(1-b_2 l_r)}{l_f+l_r} V_x(t)\right] u_1 \\ &+ \left[\frac{(-1-b_2 l_f)}{l_f+l_r} V_x(t)\right] u_2 \\ &+ \frac{(1-b_2 l_r)}{l_f+l_r}\delta_f(t) V_x(t) + a_2(V_x(t)), \end{aligned} \tag{37}$$

$$\begin{aligned} h_3(\hat{x},t) &= -b_3 V_y + r + \left[\frac{(1-b_3 l_r)}{l_f+l_r} V_x(t)\right] u_1 \\ &+ \left[\frac{(-1-b_3 l_f)}{l_f+l_r} V_x(t)\right] u_2 \\ &+ \frac{(b_3 l_r-1)}{l_f+l_r}\delta_f(t) V_x(t) + a_3(V_x(t)), \end{aligned} \tag{38}$$

$$\begin{aligned} h_4(\hat{x},t) &= -b_4 V_y + r + \left[\frac{(1-b_4 l_r)}{l_f+l_r} V_x(t)\right] u_1 \\ &+ \left[\frac{(-1-b_4 l_f)}{l_f+l_r} V_x(t)\right] u_2 \\ &+ \frac{(b_4 l_r-1)}{l_f+l_r}\delta_f(t) V_x(t) + a_4(V_x(t)). \end{aligned} \tag{39}$$

Taking the first boundary function $h_1(\hat{x},t)$ in (36) as an example, the partial derivatives of $h_1(\hat{x},t)$ in (35) are

$$\frac{\partial h_1(\hat{x},t)}{\partial V_y} = b_1, \tag{40}$$

$$\frac{\partial h_1(\hat{x},t)}{\partial r} = -1, \tag{41}$$

$$\frac{\partial h_1(\hat{x},t)}{\partial u_1} = \frac{(1-b_1 l_r)}{l_f+l_r} V_x(t), \tag{42}$$

$$\frac{\partial h_1(\hat{x},t)}{\partial u_2} = \frac{(-1-b_1 l_f)}{l_f+l_r} V_x(t), \tag{43}$$

and

$$\begin{aligned} \frac{\partial h_1(\hat{x})}{\partial t} &= \frac{(1-b_1 l_r) u_1}{l_f+l_r}\dot{V}_x(t) + \frac{(-1-b_1 l_f) u_2}{l_f+l_r}\dot{V}_x(t) \\ &+ \frac{(1-b_1 l_r)}{l_f+l_r}\left(\dot{V}_x(t)\delta_f(t) + V_x(t)\dot{\delta}_f(t)\right) \\ &+ \dot{a}_1(V_x(t)). \end{aligned} \tag{44}$$

Substituting (40)–(44) into (35) yields

$$\begin{aligned} L_f h_1(\hat{x},t) &= b_1 f_1(\hat{x}) + (-1) f_2(\hat{x}) + \left(\frac{V_x(t)(1-b_1 l_r)}{l_f+l_r}\right)\omega_1 \\ &+ \left(\frac{V_x(t)(-1-b_1 l_f)}{l_f+l_r}\right)\omega_2 + \dot{a}_1(V_x(t)) \\ &+ \frac{(1-b_1 l_r)}{l_f+l_r}\left(\dot{V}_x(t)\delta_f(t) + V_x(t)\dot{\delta}_f(t)\right) \\ &+ \frac{(1-b_1 l_r) u_1}{l_f+l_r}\dot{V}_x(t) + \frac{(-1-b_1 l_f) u_2}{l_f+l_r}\dot{V}_x(t). \end{aligned} \tag{45}$$

The final constraint for $h_1(\hat{x},t)$ is obtained by substituting (45) into (34). For the other three boundary functions $h_j(\hat{x},t), j = 2, 3, 4$, the same procedure can be applied.

As described in Proposition 1, the control design, which ensures that the inequalities in (34) are always satisfied, can guarantee system stability/safety. The key issue of solving this guaranteed stability control problem is the determination ω_1 and ω_2 in (45). Instead of directly applying u_1 and u_2 as the control inputs, we consider ω_1 and ω_2 as the virtual control inputs, which, by integration, will give u_1 and u_2 as the real control inputs of the vehicle lateral dynamics in (15). Note that in addition to the constraint derived for the first boundary function as an example, the determination of ω_1 and ω_2 should also satisfy the constraints derived with respect to the other three boundary functions in (37)–(39).

Based on all the constraints that guarantee vehicle lateral stability, a QP problem is formulated to calculate the optimal virtual control inputs. Specifically, for a given stability region as a TVCD set, the four time-varying CDBFs and the corresponding constraints can be integrated with a QP problem as follows:

$$\dot{u}(\hat{x},t) = \underset{\dot{u}\in\mathbb{R}^2}{\operatorname{argmin}} \frac{1}{2}\dot{u}^T H \dot{u} + F^T \dot{u}, \tag{46}$$

s.t.

$$\begin{aligned} &\frac{\partial h_j(\hat{x},t)}{\partial x} f(\hat{x}) + \sum_{j=1}^{4}\frac{\partial h_j(\hat{x},t)}{\partial u}\dot{u} + \frac{\partial h_j(\hat{x},t)}{\partial t} + \\ &+ \alpha_j(h_j(\hat{x},t)) \geq 0, j = 1, 2, 3, 4, \end{aligned} \tag{47}$$

$$\begin{aligned} \dot{u}_1 \in \Omega_1(u_1) &= [\dot{u}_{1,\min}, \dot{u}_{1,\max}], \dot{u}_2 \in \Omega_2(u_2) \\ &= [\dot{u}_{2,\min}, \dot{u}_{2,\max}], \end{aligned} \tag{48}$$

$$\begin{aligned} \dot{u}_{1,\max} &= 0, if\ u_1 = u_{1,\max}, \\ \dot{u}_{1,\min} &= 0, if\ u_1 = u_{1,\min}, \\ \dot{u}_{2,\max} &= 0, if\ u_2 = u_{2,\max}, \\ \dot{u}_{2,\min} &= 0, if\ u_2 = u_{2,\min}, \end{aligned} \tag{49}$$

where $\dot{u} = [\dot{u}_1\ \dot{u}_2]^T = [\omega_1\ \omega_2]^T$ denotes the virtual control inputs, $\dot{u}_{1,\max} = \dot{u}_{2,\max} = \frac{T_{\max}}{I_S}$ and $\dot{u}_{1,\min} = \dot{u}_{2,\min} = -\dot{u}_{1,\max}$ in (48), $H \in \mathbb{R}^{2\times 2}$ is positive definite, and $F \in \mathbb{R}^2$. Note that in (47), the constraints are written with respect to the virtual control inputs, where the real control u_1 and u_2 are treated as the state variables. α_j are appropriately selected class

TABLE I
VEHICLE AND SIMULATION PARAMETERS

Symbol	Parameters	Values
m_v	Vehicle mass	1270 kg
I_z	Yaw inertia	1500 kg·m^2
l_f	Front wheelbase	1.11 m
l_r	Rear wheelbase	1.8 m
$\alpha_1(x)$ & $\alpha_3(x)$	Class K function	$20x$
$\alpha_2(x)$ & $\alpha_4(x)$	Class K function	$100x$
k_1	Scaling factor	0.024
k_2	Scaling factor	0.028
H	Weighting matrix	$\begin{bmatrix} 50 & 0 \\ 0 & 50 \end{bmatrix}$
F	Weighting matrix	$[0 \quad 0]$
T_{max}	Maximum steering torque	24 Nm
$u_{1,min/max}$	Min/Max front wheel steering angle	±0.6rad(34°)
$u_{2,min/max}$	Min/Max rear wheel steering angle	±0.1rad(5.7°)
I_s	Moment of inertia of the steering system	3 kgm^2
ε	Slack number	0.01
k	Bounds on disturbances	0.1

K functions based on the sharing property among multiple CBFs [15]. The sharing property ensures the feasibility of the QP problem when multiple invariance conditions are applied. Note that, the constraints in (48) and (49) are not considered in the sharing property but simply considered as the upper and lower bounds of the control input. Specifically, the constraints in (48) denote the upper and lower limits of $\dot{u}$, which, in practice, are the steering rate bounds determined by the maximum torque of the steering motor $T_{\max}$ and the moment of inertia of the steering system I_S. The constraints in (49) ensure $u_1 \in U_1$ and$u_2 \in U_2$, where $U_1 = [u_{1,\min}, u_{1,\max}]$ and $U_2 = [u_{2,\min}, u_{2,\max}]$ denote the feasible control input sets. For vehicle systems, such feasible sets can be determined by the mechanical structures of steering systems.

Remark 7 (Proof of feasibility): Following the feasibility discussions in [16], the optimization in (46)–(49) is feasible if the vector field of system dynamics in (15) and the TVCDBF in (36)–(39) are locally Lipschitz with the assumption of a non-zero V_x. The feasibility can also be guaranteed based on the sharing property among multiple invariant constraints [15]. As shown in Table I, the Class K functions for h_1 and h_3 are selected as the same and the Class K functions for h_2 and h_4 are selected as the same. For the boundaries that have an intersection (e.g., h_2 and h_3), different class K functions are selected. The system dynamics, barrier functions, and Class K functions adopted in this paper satisfy the required conditions. Therefore, the feasibility of QP in (46)–(49) can be guaranteed.

After the optimal virtual control $\dot{u}$ are obtained, the real control inputs u are then determined by integration. It is also worth noting that by integrating $\dot{u}_1$ and $\dot{u}_2$, we have u_1 and u_2 at the current time, which gives us a priori information to decide whether or not to include any of the constraints in (49). Hence, the problem is still a QP at run-time. Finally, in vehicle systems, u_1 is typically combined with δ_f as the total front wheel steering angle. A framework of the proposed guaranteed vehicle lateral stability control using time-varying CDBF is shown in Fig. 3 .

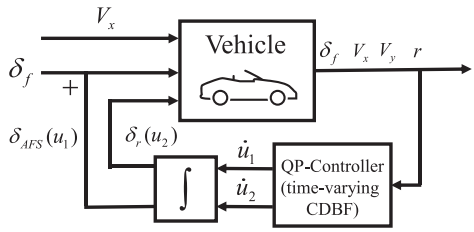

Fig. 3. Framework of vehicle lateral stability control.

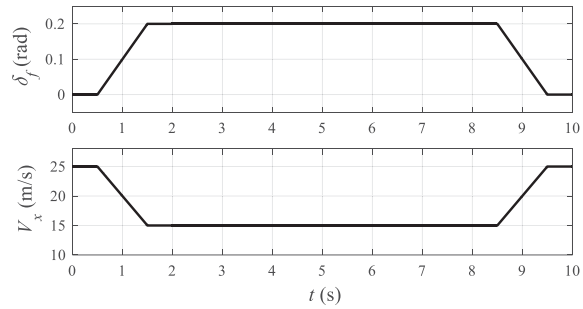

Fig. 4. Time-varying profiles (the front wheel steering angle and the longitudinal velocity) in the J-turn maneuver.

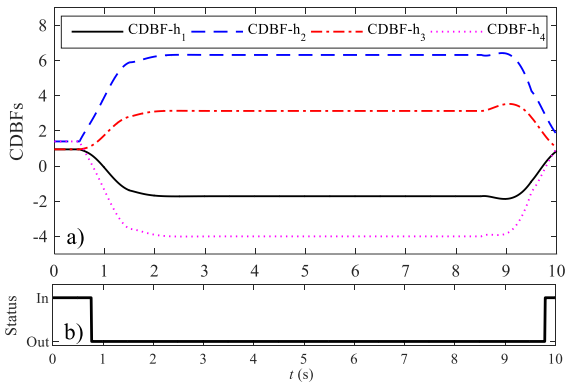

Fig. 5. Feedforward case simulation results in the J-turn maneuver, a) CDBFs values, b) vehicle stability status.

Note that during the QP implementation for the sampled system, signal delays due to the sampling may occur. Such delays could cause a short period of CDBF violation, especially when the system states are controlled close to the boundaries of the stability set. To solve this issue, in (13), a small positive slack number ε could be added to the time-varying CDBF in the extended class K function as $\alpha(h(\hat{x}, t) - \varepsilon)$. The slack number εcan be also applied to overcome possible robustness issues in practical applications. In [16], it was found that if the disturbance is vanishing or sufficiently small, the control barrier function can still guarantee the set invariance. For any bounded disturbance (e.g., $\|g\|_\infty \leq k$), by adding k to the slack number ε, set invariance can be robustly guaranteed. Although the value of k could be difficult to find *a priori* for a general disturbance, it can be estimated for specific systems and operation conditions, such as vehicle systems [43].

V. Simulation Results and Discussions

In this section, the proposed new definitions and the corresponding vehicle stability control design are verified through simulation results of high-speed J-turn and double lane change (DLC) maneuvers. The vehicle parameters shown in Table I are selected based on the database of a C-class hatchback vehicle model in CarSim. To ensure the feasibility of the QP problem (46)–(49), the selected Class *K* functions in Table I were verified by the sharing property in [15]. Specifically, as shown in Table I, the Class *K* functions for h_1 and h_3 are selected as the same and the Class *K* functions for h_2 and h_4 are selected as the same. The reason for this selection is, for h_1 and h_3, the corresponding stability region boundaries do not have intersections (the upper left and lower right boundaries of any of the three regions in Fig. 1), which reduces the possibility of conflicts. For the boundaries that have an intersection (e.g., h_2 and h_3), different Class *K* functions are selected. The real-time feasibility of the proposed control method for both scenarios below was verified by implementing the proposed control algorithm on a real vehicle test platform equipped with a dSPACE MicroAutobox II, where we observed that the computations can be completed in real-time without delays when the main processor runs at a 900MHz clock frequency.

A. High-Speed J-Turn Maneuver

Two simulation cases are conducted and compared to demonstrate the effectiveness of the control design based on the proposed time-varying CDBF. Given the same steering and longitudinal velocity profile, the first case simulates the vehicle driving behavior based on the feedforward steering angle δ_f. The second case simulates the feedback vehicle control with the guaranteed vehicle stability control design. The feedforward front wheel steering angle δ_f and the longitudinal velocity V_x are given in Fig. 4 as time-varying variables. Specifically, the time-varying functions of $\delta_f(t)$ and $V_x(t)$ are given as

$$\delta_f(t) = \begin{cases} 0.2t - 0.1\,rad & 0.5 < t \le 1.5 \\ 0.2\,rad & 1.5 < t \le 8.5 \\ -0.2t + 1.9\,rad & 8.5 < t < 9.5 \end{cases},$$

$$V_x(t) = \begin{cases} -10t + 30\,m/s & 0.5 < t \le 1.5 \\ 15\,m/s & 1.5 < t \le 8.5 \\ 10t - 70\,m/s & 8.5 < t < 9.5 \end{cases}. \quad (50)$$

Note that when the vehicle inputs are zeros, the proposed control design will not be applied since there will be no vehicle movement, i.e., $V_x(t) = 0$. In this simulation, the tire-road friction coefficient is set to 0.85 for road conditions to ensure sufficient friction forces.

In the first case, the feedback control inputs are all zeros, namely, $u_1 = u_2 = 0$. Thus, the stability region is time-varying with respect to the feedforward steering angle and vehicle longitudinal speed. As shown in Fig. 5a), negative time-varying CDBF values are clearly observed for h_1 and h_4, which indicate that the system states are not kept within the defined TVCD invariant (stability) set, as described in Definition 6. The corresponding unstable statuses are also verified by the vehicle status check results, shown in Fig. 5b). The vehicle status "in" or "out" the TVCD stability set in Fig. 5b) is checked by whether the instantaneous vehicle states are located in the TVCD stability region, which is an independent evaluation process based on the instantaneous check of state and region locations in the phase plane [28]. Moreover, the vehicle states (V_y and r) are shown in Fig. 6 for the J-turn maneuver, with relatively large values.

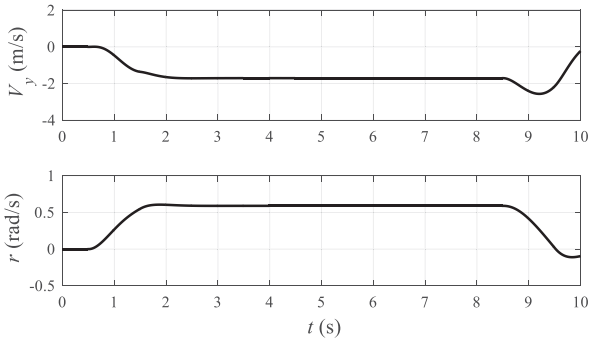

Fig. 6. Vehicle states in the J-turn maneuver: feedforward control.

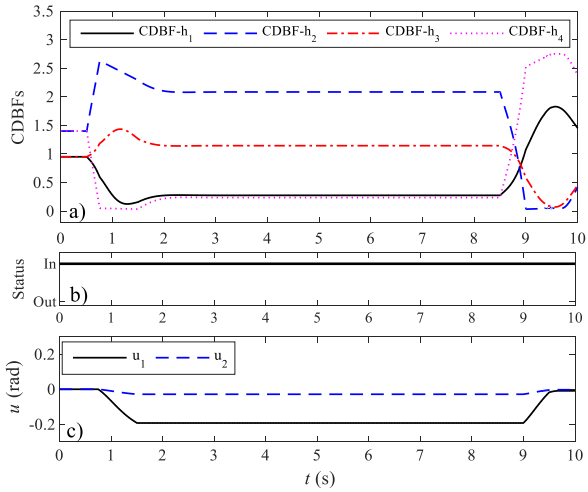

Fig. 7. Feedback case simulation results in the J-turn maneuver, a) CDBFs values, b) vehicle stability status, c) control inputs.

In the second case, the feedback front and rear wheel steering angles are calculated using the QP problem with respect to the constraints derived from the proposed time-varying CDBFs. As shown in Fig. 7a), all the four time-varying CDBFs are well controlled to be positive during the whole maneuver, which indicates that the vehicle states are always within the TVCD stability region. Since the vehicle stability region is both time-varying and control-dependent, the control design based on the proposed time-varying CDBF is verified. In Fig. 7b), the vehicle status check always shows 'in' status for the whole maneuver, which is consistent with the meaning of positive time-varying CDBF values. In Fig. 7c), the rear wheels are slightly steered to the same direction of the front wheels to keep the vehicle stable, which demonstrates the same idea that the rear wheels should turn to the same direction of the front wheels to keep a 4WS vehicle stable at high speeds [37]. In addition, by comparing

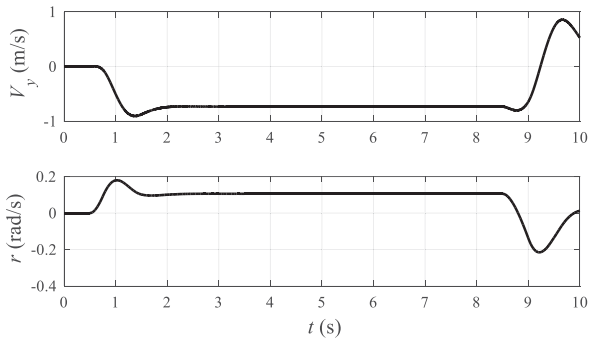

Fig. 8. Vehicle states in the J-turn maneuver: feedback control.

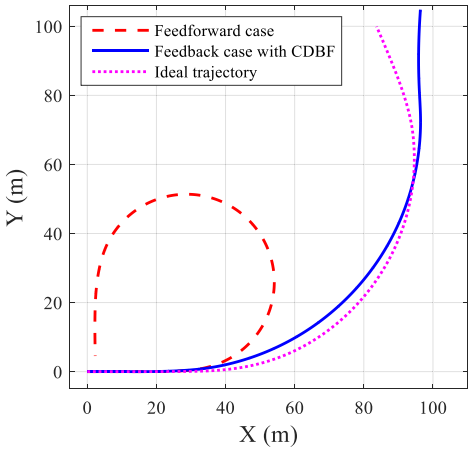

Fig. 9. Vehicle trajectories comparison in the J-turn maneuver.

the vehicle states in Fig. 8 with those in Fig. 6, V_y and r for the feedback control case are both smaller than those in the feedforward case, which indicates a more stable and safer vehicle status. Such a stability improvement can also be demonstrated by comparing the vehicle planar trajectories between these two cases. As shown in Fig. 9, the vehicle trajectory in the feedback case is much less extreme than that of the feedforward case, which could easily cause the vehicle to spin or collide with other vehicles. In Fig. 9, the desired trajectory is the path of a vehicle with an ideal tire model when the same feedforward traces in Fig. 4 are given. The tire cornering stiffness coefficients in a linear tire model are calibrated based on the nonlinear tire model in Appendix C. From the comparison shown in Fig. 4, the vehicle trajectory of feedback case with CDBF is much closer to the desired trajectory, also indicating a better vehicle driving performance.

To further verify the proposed time-varying CDBF method, another simulation is conducted by using a fixed stability region (common in literature) as the invariant set, bounded by the pink dotted lines in Fig. 10 (similar to that in Fig. 1). The four straight lines are represented by four time-invariant and control-independent barrier functions in linear forms. As observed in Fig. 10, the vehicle state trajectory is well covered by the fixed region. The four BFs, as shown in Fig. 11a), are also positive during the whole maneuver since the trajectory is always

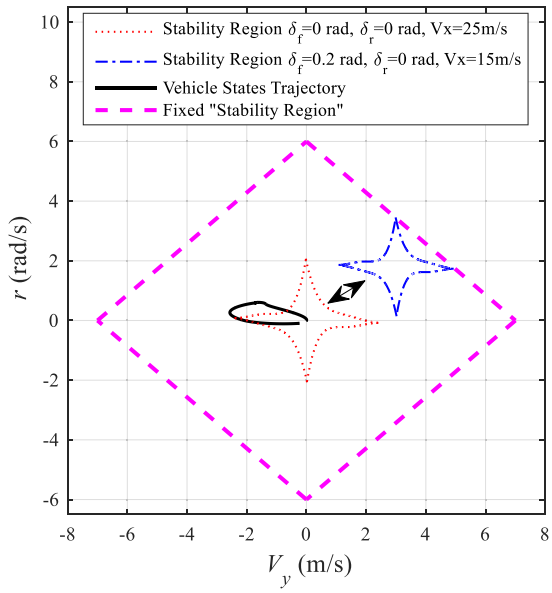

Fig. 10. Vehicle state trajectory with regard to the fixed "stability region" in the J-turn maneuver.

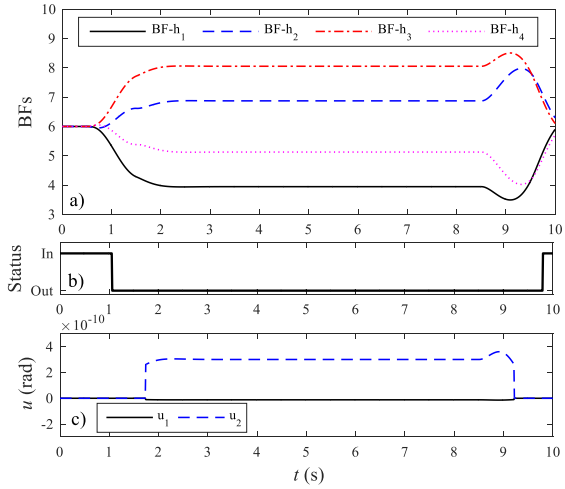

Fig. 11. Feedback case simulation results in the J-turn maneuver based on the fixed stability region, a) BFs values, b) vehicle stability status, c) control inputs.

in the fixed region. Moreover, since the vehicle state trajectory is far away from the boundaries, the feedback control inputs, as shown in Fig. 11c), are pretty small and negligible. Such small feedback control inputs barely influence the vehicle dynamics, and thus the vehicle states are very similar to those shown in Fig. 6 in the feedforward simulation. However, as mentioned in Remark 4, the fixed region is too large to precisely describe vehicle stability. By checking the vehicle status with respect to the TVCD stability region, as shown in Fig. 11b), it is revealed that the vehicle is not always "in" the stability region. This observation demonstrates that using the fixed stability region as the invariant set cannot guarantee vehicle stability.

Note that since the fixed stability region is not control-dependent, the stability constraints do not contain $\dot{u}$. In such

TABLE II
PARAMETERS OF NOISE IN SIMULATIONS

Noise	Noise level (in percent of nominal values)	Frequency
V_y	5%	200 Hz
r	5%	200 Hz
V_x	3%	200 Hz
δ_f	3%	200 Hz

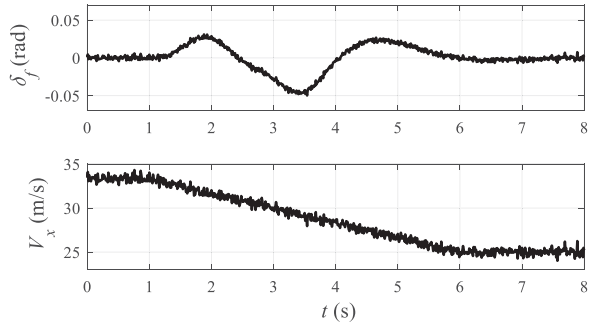

Fig. 12. Time-varying profiles (the front wheel steering angle and the longitudinal velocity) in the DLC maneuver.

a case, the control input u is selected as the control variable in the QP, where the constraints in (48) and (49) are not applied.

B. Double Lane Change Maneuver

A double lane change maneuver is a commonly adopted scenario for the test of vehicle stability in extreme conditions. From a practical point of view, to verify the robustness of the proposed control method, measurement and estimation noises on vehicle states are added in the simulation. The parameters of the added noise signals (listed in Table II) are determined based on experimental data [44], [45]. All noise signals are assumed to follow a Gaussian probability distribution with a frequency of 200 Hz. In this simulation, the tire-road friction coefficient is set to 0.5 to simulate wet road conditions. Similar to the J-turn maneuver, two simulation cases (feedforward and feedback cases) are conducted and compared. As shown in Fig. 12, the profiles of the front wheel steering angle and the longitudinal velocity are given as two time-varying variables. Note that the longitudinal velocity is intentionally selected to be larger than 25 m/s to illustrate the generality of the proposed method.

In the feedforward case, the stability region is varying with respect to the feedforward steering angle and vehicle longitudinal speed. As shown in Fig. 13a), negative CDBF values are clearly observed, indicating that the system states are out of the TVCD stability region. Such unstable statuses are also verified by the vehicle status check shown in Fig. 13b).

In the feedback case, the vehicle is controlled by the proposed stability controller. All four time-varying CDBFs, as shown in Fig. 14a), are positive, indicating that the vehicle states are always controlled to stay within the TVCD stability region. Since the vehicle stability region is both time-varying and

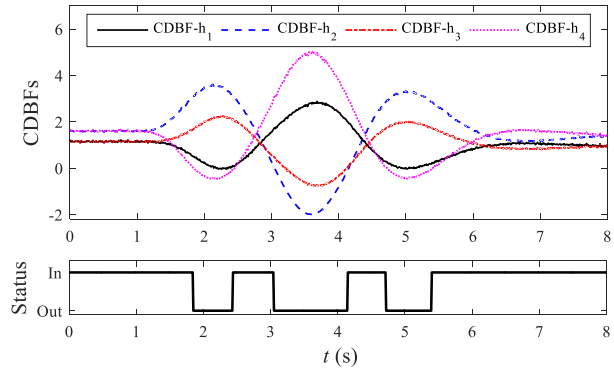

Fig. 13. Feedforward case simulation results in the DLC maneuver, a) CDBFs values, b) vehicle stability status.

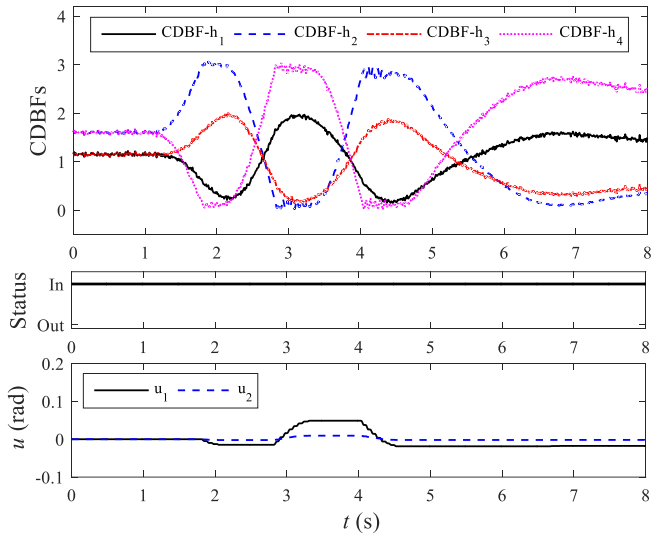

Fig. 14. Feedback case simulation results in the DLC maneuver, a) CDBFs values, b) vehicle stability status, c) control inputs.

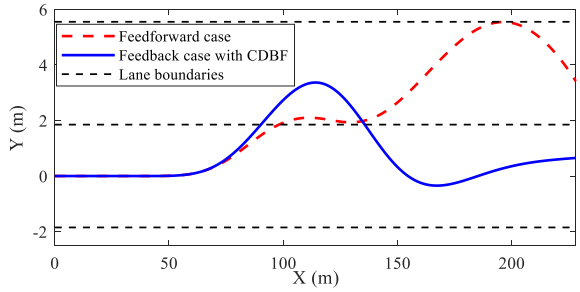

Fig. 15. Vehicle trajectories comparison in the DLC maneuver.

control-dependent, the control design based on the proposed time-varying CDBF is verified. In Fig. 14b), the vehicle statuses are always 'in' the stability region during the whole maneuver, which is consistent with the meaning of all four positive CDBF values. In Fig. 14c), the real control inputs u after the integration of the virtual control $\dot{u}$ are presented.

The stability improvement is also demonstrated by comparing the vehicle planar trajectories. As shown in Fig. 15, with only feedforward control, the vehicle cannot complete a DLC maneuver due to the loss of stability on a slippery road. However, with the proposed stability control design, the vehicle is able to successfully realize the DLC maneuver.

VI. Conclusion

This paper presents a new concept of a TVCD invariant set and a novel control algorithm to guarantee the invariance of a TVCD set. By involving the TVCD properties, the proposed time-varying CDBF is more general than the (time-varying) CBFs studied in the literature. The newly developed theory and control methods are applied to solve a guaranteed region-based vehicle lateral stability control problem, where the vehicle lateral stability region, as the controlled invariant set, is both time-varying and control-dependent. Finally, through realistic simulation results of high-speed J-turn and DLC maneuvers, the proposed new concepts and control design are verified.

Appendix

The complete proof of Proposition 1 is given as follows.

A. Proof of the TVCD Invariant Set Using the Time-Varying ZCDBF

Based on the definition of the tangent cone [42] and Nagumo's theorem [7], the invariance condition in (13) indicates that when $x \in \partial\psi$, the derivative $\dot{x}$ points inside or is tangent to ψ [7], then the trajectory $x(t)$ remains in ψ. Thus, if the system state is initially in the set, it then follows that the system state is always kept inside the set and $h(\hat{x}, t) > 0$. According to (10), if $h(\hat{x}, t) \geq 0$, $x \in \psi(u, t)$ for all $u \in U$and $t \in T$ is proved, which indicates that the $\psi(u, t)$ is a TVCD invariant set. ■

B. 2D LuGre Tire Model

A 2D LuGre tire model is described as in [38] as follows:

$$\begin{aligned} F_y &= f\left(\lambda, \alpha_{f,\,r}, F_n, \mu\right) \\ &= F_n \left\{ \frac{g_i^2 v_{ri}}{\gamma\left(v_r, \mu\right)} \left[1 - \frac{\beta_i}{a_i^2} \left(\frac{e^{-a_i L_i} - e^{-a_i (L_i - \zeta_{Li})}}{\zeta_{Li}} - \right. \right. \right. \\ &\quad \left. \left. \left. - \frac{e^{-a_i (L_i - \zeta_{Ri})} - 1}{L_i - \zeta_{Ri}} \right) \right] + \sigma_{2i} v_{ri} \right\}, \end{aligned} \tag{51}$$

where $\lambda, \alpha_{f,\,r}, F_n$, and μ are the tire slip ratio, front or rear wheel slip angle, vertical load, and friction coefficient, respectively. The parameters in the curly brackets are calibrated based on the CarSim tire database to describe the Stribeck effect, trapezoidal load distribution, and the viscous damping property of tire materials. The definitions of the rest of the parameters in (51) $(g_i, v_{ri}, v_r, \beta_i, a_i, L_i, \zeta_{Li}, \zeta_{Ri}, \sigma_{2i})$ and more details about the nonlinear and coupled LuGre tire model can be found in [38].

References

[1] B. Paden, M. Čáp, S. Z. Yong, D. Yershov, and E. Frazzoli, "A survey of motion planning and control techniques for self-driving urban vehicles," *IEEE Trans. Intell. Veh.*, vol. 1, no. 1, pp. 33–55, Mar. 2016.

[2] On-Road Automated Driving (ORAD) committee, Taxonomy and definitions for terms related to driving automation systems for on-road motor vehicles, SAE International, Jun. 2018.

[3] K. D. Kim and P. R. Kumar, "An MPC-based approach to provable system-wide safety and liveness of autonomous ground traffic," *IEEE Trans. Autom. Control*, vol. 59, no. 12, pp. 3341–3356, Dec. 2014.

[4] P. Ogren and N. E. Leonard, "A convergent dynamic window approach to obstacle avoidance," *IEEE Trans. Robot.*, vol. 21, no. 2, pp. 188–195, Apr. 2005.

[5] S. Prajna, "Optimization-based methods for nonlinear and hybrid systems verification," Ph.D. thesis, California Inst. Technl., Pasadena, CA, USA, 2005.

[6] S. Prajna and A. Jadbabaie, "Safety verification of hybrid systems using barrier certificates," in *Hybrid Systems: Computation and Control*. Berlin, Germany: Springer-Verlag, pp. 477–492, 2004.

[7] F. Blanchini, "Set invariance in control," *Automatica*, vol. 35, pp. 1747–1767, 1999.

[8] P. Wieland and F. Allgöwer, "Constructive safety using control barrier functions," in *Proc. IFAC Nonlinear Control Syst.*, 2007, pp. 473–478.

[9] A. D. Ames, X. Xu, J. W. Grizzle, and P. Tabuada, "Control barrier function based quadratic programs for safety critical systems," *IEEE Trans. Autom. Control*, vol. 62, no. 8, pp. 3861–3876, Aug. 2017.

[10] K. B. Ngo, R. Mahony, and Z. Jiang, "Integrator backstepping using barrier functions for systems with multiple state constraints," in *Proc. IEEE Conf. Decis. Control*, 2005, pp. 8306–8312.

[11] K. P. Tee, S. S. Ge, and E. H. Tay, "Barrier lyapunov functions for the control of output-constrained nonlinear systems," *Automatica*, vol. 45, no. 4, pp. 918–927, 2009.

[12] K. P. Tee, B. Ren, and S. S. Ge, "Control of nonlinear systems with time-varying output constraints," *Automatica*, vol. 47, pp. 2511–2516, 2011.

[13] W. He, C. Sun, and S. S. Ge, "Top tension control of a flexible marine riser by using integral-barrier lyapunov function," *IEEE Trans. Mechatronics*, vol. 20, no. 2, pp. 497–505, Apr. 2015.

[14] Y. Liu and S. Tong, "Barrier Lyapunov functions-based adaptive control for a class of nonlinear pure-feedback systems with full state constraints," *Automatica*, vol. 64. pp. 70–75, 2016.

[15] X. Xu, "Constrained control of input-output linearizable system using control sharing barrier functions," *Automatica*, vol. 87, pp. 195–201, 2018.

[16] X. Xu, P. Tabuada, J. W. Grizzle, and A. D. Ames, "Robustness of control barrier functions for safety critical control," in *Proc. IFAC Conf. Anal. Des. Hybrid Syst.*, 2015, pp. 54–61.

[17] X. Xu, J. W. Grizzle, P. Tabuada, and A. D. Ames, "Correctness guarantees for the composition of lane keeping and adaptive cruise control," *IEEE Trans. Automat. Sci. Eng.*, vol. 15, no. 3, pp. 1216–1229, Jul. 2018.

[18] Y. Chen, H. Peng, and J. Grizzle, "Obstacle avoidance for low-speed autonomous vehicles with barrier function," *IEEE Trans. Control Syst. Technol.*, vol. 26. no. 1, pp. 194–206, Jan. 2018.

[19] L. Wang, A. D. Ames, and M. Egerstedt, "Safety barrier certificates for collision multirobot system," *IEEE Trans. Robot.*, vol. 33, no. 3. pp. 661–674, Jun. 2017.

[20] S. Grammatico, F. Blanchini, and A. Caiti, "Control-sharing and merging control Lyapunov functions," *IEEE Trans. Autom. Control*, vol. 59, no. 1, pp. 107–119, Jan. 2014.

[21] M. Z. Romdlony and B. Jayawardhana, "Stabilization with guaranteed safety using control lyapunov-barrier function," *Automatica*, vol. 66, pp. 39–47, 2016.

[22] G. Fan and K. Sreenath, "Safety-critical and constrained geometric control synthesis using control lyapunov and control barrier functions for systems evolving on manifolds," in *Proc. Amer. Control Conf.*, pp. 2038–2044, 2015.

[23] M. Jankovic, "Combining control lyapunov and barrier functions for constrained stabilization of nonlinear systems," in *Proc. IEEE Amer. Control Conf.,* pp. 1916–1922, 2017.

[24] Z. Wu, F. Albalawi, Z. Zhang, J. Zhang, H. Durand, and P. D. Christofides, "Control Lyapunov-barrier function-based model predictive control of nonlinear systems," *Automatica*, vol. 109, 2019, Art. no. 108508.

[25] Z. Wu and P. D. Christofides, "Control Lyapunov-barrier function-based predictive control of nonlinear processes using machine learning modeling," *Comput. Chem. Eng.*, vol. 134, 2020, Art. no. 106706.

[26] L. Lindemann and D. V. Dimarogonas, "Control barrier functions for signal temporal logic tasks," *IEEE Control Syst. Lett.*, vol. 3, no. 1, pp. 96–101, Jan. 2019.
[27] M. Kimmel and S. Hirche, "Invariance control for safe human-robot interaction in dynamic environments," *IEEE Trans. Robot.*, vol. 33, no. 6. pp. 1327–1342, Dec. 2017.
[28] Y. Huang and Y. Chen, "Estimation and analysis of vehicle lateral stability region with both front and rear wheel steering," in *Proc. ASME Dyn. Syst. Control Conf.*, No. DSCC2017-5154, Tysons, VA, USA, 2017.
[29] E. Ono, S. Hosoe, H. D. Tuan, and S. Doi, "Bifurcation in vehicle dynamics and robust front wheel steering control," *IEEE Trans. Control Syst. Technol.*, vol. 6, no. 3, pp. 412–420, May 1998.
[30] Y. Huang, W. Liang, and Y. Chen, "Stability regions of vehicle lateral dynamics: Estimation and analysis," *ASME J. Dyn. Syst., Meas. Control*, vol. 143, no. 5, 2021, Art. no. 051002.
[31] Y. Huang, S. Z. Yong, and Y. Chen, "Guaranteed vehicle safety control using control-dependent barrier functions," in *Proc. Amer. Control Conf.*, pp. 983–988, Philadelphia, PA, USA, 2019.
[32] H. K. Kahlil, *Nonlinear Systems*. Upper Saddle River, NJ, USA: Prentice Hall, 2002.
[33] L. Kocarev, U. Parlitz, and B. Hu, "Lie derivatives and dynamical systems," *Chaos, Solitons Fractals*, vol. 9, no. 8, pp. 1359–1366, 1998.
[34] E. Mousavinejad, Q. Han, F. Yang, Y. Zhu, and L. Vlacic "Integrated control of ground vehicles dynamics via advanced terminal sliding mode control," *Veh. Syst. Dyn.*, vol. 55, no. 2, pp. 268–294, 2017.
[35] C. G. Bobier and J. C. Gerdes, "Staying within the nullcline boundary for vehicle envelope control using a sliding surface," *Veh. Syst. Dyn.*, vol. 51, no. 2, pp. 199–217, 2013.
[36] H. Jeffreys and B. S. Jeffreys, *Methods of Mathematical Physics*. Cambridge, U.K.: Cambridge Univ. Press, 1988.
[37] Y. Furukawa, N. Yuhara, S. Sano, H. Takeda, and Y. Matsushita, "A review of four-wheel steering studies from the viewpoint of vehicle dynamics and control," *Veh. Syst. Dyn.*, vol. 18, pp. 151–186, 1989.
[38] W. Liang, J. Medanic, and R. Ruhl, "Analytical dynamic tire model," *Veh. Syst. Dyn.*, vol. 46, no. 3, pp. 197–227, 2008.
[39] S. Inagaki, I. Kushiro, and M. Yamamoto, "Analysis on vehicle stability in critical cornering using phase-plane method," *JSAE Rev.*, vol. 16, no. 2, pp. 287–292, 1995.
[40] S. Sadri and C. Wu, "Stability analysis of a nonlinear vehicle model in plane motion using the concept of lyapunov exponents," *Veh. Syst. Dyn.*, vol. 51, no. 6, pp. 906–924, 2013.
[41] R. P. Agarwal, R. P. Agarwal, and V. Lakshmikantham, *Uniqueness and Nonuniqueness Criteria For Ordinary Differential Equations*, Singapore: World Scientific, vol. 6, 1993.
[42] J. P. Aubin and H. Frankowska, *Set-Valued Analysis*. Boston, MA, USA: Birkhauser, 1990.
[43] C. Funfschilling and G. Perrin, "Uncertainty quantification in vehicle dynamics," *Veh. Syst. Dyn.*, vol. 57, no. 7, pp. 1062–1086, 2019.
[44] A. Rezaeian, A. Khajepour, W. Melek, S.-K. Chen, and N. Moshchuk, "Simultaneous vehicle real-time longitudinal and lateral velocity estimation," *IEEE Trans. Veh. Technol.*, vol. 66, no. 3, pp. 1950–1962, Mar. 2017.
[45] X. Wang, *Vehicle Noise and Vibration Refinement*. Cambridge, U.K.: Woodhead Publishing Limited, 2010.

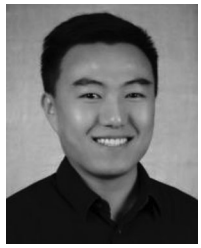

Yiwen Huang received the B.S. and M.S. degrees in mechanical engineering from Xi'an Jiaotong University, Xi'an, China, and Arizona State University, Tempe, AZ, USA, in 2014 and 2016, respectively. He is currently working toward the Ph.D. degree in mechanical engineering with Arizona State University. His research interests focused on the development of autonomous vehicle and applications, vehicle dynamics and control, mechanical design and modeling, and optimization.

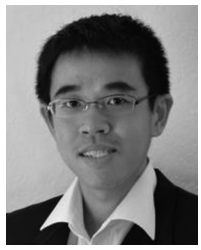

Sze Zheng Yong (Member, IEEE) is an Assistant Professor with the School for Engineering of Matter, Transport and Energy, Arizona State University. He received the Dipl.-Ing.(FH) degree in automotive engineering with a specialization in mechatronics and control systems from the Esslingen University of Applied Sciences, Germany in 2008, and the S.M. and Ph.D. degrees in mechanical engineering from the Massachusetts Institute of Technology, Cambridge, MA, USA, in 2010 and 2016, respectively. His research interests include the broad areas of control, estimation, planning, identification and analysis of hybrid systems, with applications to autonomous, robotic and cyber-physical dynamic systems and their safety, robustness and resilience. He was the recipient of a DARPA Young Faculty Award in 2018 as well as NSF CAREER and NASA Early Career Faculty awards in 2020.

Yan Chen (Member, IEEE) received the B.S. and M.S. degrees (with Hons.) in control science and engineering from the Harbin Institute of Technology, Harbin, China in 2004 and 2006, respectively. He received his second M.S. degree in mechanical engineering from the Rice University, Houston in 2009, and the Ph.D. degree in mechanical engineering from the Ohio State University, Columbus in 2013.

Dr. Chen joined Arizona State University as an Assistant Professor in 2016, after three years of full-time automotive industrial research experience. He has the authored or coauthored more than 55 peer-reviewed publications. His research interests include design, modeling, estimation, control and optimization of dynamic systems, specifically for connected and automated vehicle, electric vehicle, internal combustion engine, powertrain, aftertreatment, energy, and mechatronic systems.

Dr. Chen is as an Associate Editor for IEEE TRANSACTIONS ON VEHICULAR TECHNOLOGY, *IFAC Mechatronics*, ASME Dynamic Systems and Control Conference (DSCC), and American Control Conference. He is the Vice Chair of ASME Automotive and Transportation Systems Technical Committee since 2020. He was the recipient of 2020 SAE Ralph R. Teetor Educational Award and 2019 DSCC Automotive and Transportation Systems Best Paper Award.